SCIENCE CHINA
Earth Sciences

SPECIAL TOPIC: China since the Last Glacial Maximum
•RESEARCH PAPER•

August 2019 Vol.62 No.8: 1269–1278
https://doi.org/10.1007/s11430-018-9338-3

Quantitative climatic reconstruction of the Last Glacial Maximum in China

Haibin WU[1,2,3*], Qin LI[1,4], Yanyan YU[1], Aizhi SUN[3], Yating LIN[1,3], Wenqi JIANG[1,3] & Yunli LUO[5]

[1] *Key Laboratory of Cenozoic Geology and Environment, Institute of Geology and Geophysics, Chinese Academy of Sciences, Beijing 100029, China;*
[2] *CAS Center for Excellence in Life and Paleoenvironment, Beijing 100044, China;*
[3] *University of Chinese Academy of Sciences, Beijing 100049, China;*
[4] *CAS Center for Excellence in Tibetan Plateau Earth Sciences, Beijing 100101, China;*
[5] *Institute of Botany, Chinese Academy of Sciences, Beijing 100093, China*

Received September 3, 2018; revised January 10, 2019; accepted February 13, 2019; published online March 25, 2019

Abstract Quantitative paleoclimatic reconstruction is crucial for understanding the operation and evolution of the global climate system. For example, a quantitative paleoclimatic reconstruction for the Last Glacial Maximum (18±2 ka ^{14}C, LGM) is fundamental to understanding the evolution of Earth's climate during the last glacial-interglacial cycle. Previous quantitative palaeoclimate reconstructions in China are generally based on statistical comparison of modern pollen assemblages and modern climate data. These methods are based on the premise that vegetation-climate interactions remain the same through time, and implicitly assume that the interactions are independent of changes in seasonality and atmospheric CO_2 concentration. However, these assumptions may not always be valid, which may affect the reconstructions. Here, we present the results of a quantitative study of the LGM climate of China based on an improved inverse vegetation model which incorporates physiological processes combined with a new China Quaternary Pollen Database. The results indicate that during the LGM, mean annual temperature (ANNT), mean temperature of the coldest month (MTCO) and mean temperature of the warmest month in China were lower by ~5.6±0.8, ~11.0±1.6 and ~2.6±0.9°C, respectively, compared to today, and that the changes in ANNT were mainly due to the decrease of MTCO. The ANNT decrease in southern China was ~5.5±0.5°C. Mean annual precipitation was lower by ~46.3±17.8 mm compared to today and was especially low in northern China (~51.2±21.4 mm) due to the decrease in summer rainfall. Comparison of our results with recent outputs from paleoclimatic modelling reveals that while the latter are broadly consistent with our estimated changes in mean annual climatic parameters, there are substantial differences in the seasonal climatic parameters. Our results highlight the crucial importance of developing seasonal simulation on paleoclimatic models, as well as the need to improve the quality of paleoclimatic reconstructions based on proxy records from geological archives.

Keywords Quantitative paleoclimatic reconstruction, Inverse vegetation model, Biome, Seasonal climate changes, Atmospheric CO_2 concentration

Citation: Wu H, Li Q, Yu Y, Sun A, Lin Y, Jiang W, Luo Y. 2019. Quantitative climatic reconstruction of the Last Glacial Maximum in China. Science China Earth Sciences, 62: 1269–1278, https://doi.org/10.1007/s11430-018-9338-3

1. Introduction

Quantitative paleoclimatic reconstruction is a key objective of paleoclimatic research, and is crucial for understanding the evolution of Earth's climate and for reducing the uncertainty of future climate predictions (IPCC, 2013). The Last Glacial Maximum (LGM, 18±2 ka ^{14}C), was an interval of extremely cold and dry conditions when global ice volume

* Corresponding author (email: Haibin-wu@mail.iggcas.ac.cn)

was at a maximum, greenhouse gas concentrations were lower than today, and terrestrial vegetation and land surface characteristics were significantly different from today (CLIMAP Project Members, 1976; Bartlein et al., 2010). However, insolation was similar to the present and therefore the LGM is well suited for evaluating climate model performance (Joussaume and Taylor, 1999; Crucifix et al., 2012; Kageyama et al., 2017).

During the past few decades, a primary global/regional paleo-dataset representing the spatial climatic pattern of the LGM has been assembled. It represents a major research effort in the field of quantitative paleoclimatic reconstruction (CLIMAP Project Members, 1976; Farrera et al., 1999; MARGO Project Members, 2009; Bartlein et al., 2010), and enables comparison with model simulations (Pinot et al., 1999; Otto-Bliesner et al., 2009; Braconnot et al., 2012; Harrison et al., 2015). This reconstruction is crucial for evaluating changes in the Earth's climate system on different time scales, and it provides an opportunity to examine the dynamic mechanisms underpinning the changes. However, Earth's climate system exhibits a spatially varying response to changes in the underlying land surface and atmospheric CO_2 concentrations. In addition, previous reconstructions were focused on Europe and North America (Peyron et al., 1998; Webb et al., 1998; Bartlein et al., 2011; Izumi and Bartlein, 2016), and it is important to extend paleoclimatic reconstruction to other regions, in order to better understand the Earth's climate system during the LGM.

China has an extended terrestrial surface with strong spatial climatic variability, which is mainly controlled by the East Asian monsoon, together with the topography; thus, it is an important region for understanding the history of East Asian monsoon circulation during glacial-interglacial periods. Much research has been conducted in the areas of quantitative paleoclimatic reconstruction for China, based on pollen-climate transfer functions (e.g. Song and Sun, 1997; Chen et al., 2015), the response surface method (e.g., Sun et al., 1996) and the modern analog method (e.g. Zheng and Guiot, 1999). The results indicate that cold conditions prevailed over China during the LGM, and that the magnitude of the decrease in annual mean temperature (ANNT) varied from ~8–10°C (Jiang et al., 2011) spatially. By contrast, the magnitude of the decrease in LGM temperatures reconstructed using the biomarker method (i.e. UK^{37}, GDGTs) is significantly less than that reconstructed using pollen data; for example, the temperature decrease in the southern China was only ~3–5°C (Chu et al., 2017; Wang et al., 2017). In addition, there is a divergence between paleoclimatic reconstructions and model simulations; the modelled decrease in the ANNT of China was only ~4.5°C (Jiang et al., 2011; Tian and Jiang, 2016), much lower than that estimated by proxy-based reconstructions.

The origin of these discrepancies between modelled and proxy data remains unclear, and thus it is important to improve the reliability of paleoclimatic reconstructions based on geological records, as well as to develop improved model simulations. Previous reconstructions are based on the assumption that vegetation-climate interactions remain constant through time, with the implicit assumption that these interactions are independent of changes in seasonal climate and atmospheric CO_2 concentration. However, these assumptions may lead to results that are substantially biased, for the following reasons: (1) Since plant growth is mainly controlled by climatic conditions during the growing season, paleoclimatic reconstructions may reflect seasonal conditions rather than the mean annual climate state (Liu et al., 2014). (2) Past seasonal climate variations may be outside the modern observed climate space, and pollen assemblages lacking modern analogs are documented during glacial periods (Peyron et al., 1998; Jackson and Williams, 2004; Guiot et al., 2008). (3) The atmospheric CO_2 concentration at the LGM was only ~200 ppmv (1 ppmv=1 mg/L), significantly lower than today (EPICA community members, 2004); and because vegetation-climate interactions are sensitive to atmospheric CO_2 levels, some vegetation changes may be due to the low atmospheric CO_2 level itself, rather than to climate change (Jolly and Haxeltine, 1997; Street-Perrott et al., 1997). The studies referenced above suggest that previous pollen-based estimates of climate change during the LGM may have a higher degree of uncertainty than commonly realized. Thus, a new approach combined with appropriate data is necessary to address these issues.

The study presented herein has two important aspects: we use an improved inverse vegetation modeling approach with a physiological process-based vegetation model, including seasonal climate changes and the effect of atmospheric CO_2 on plant growth (Guiot et al., 2000; Wu et al., 2007a, 2016); and a new China Quaternary Pollen Database. Our aim is to provide better spatial and quantitative seasonal climate estimates from pollen records, and thus to improve our understanding of the mechanisms of responsible for the climate of China at the LGM.

2. Data and methods

2.1 Pollen data

Fossil pollen records provide evidence of changes in vegetation distribution over time. In the last two decades, numerous high-resolution LGM and Holocene pollen records with high-precision dating have been obtained from China. These records provide a good opportunity to reconstruct the spatiotemporal distribution of vegetation and climate in China. In this study, we assembled fossil pollen data sets from publications, and augmented the Chinese Quaternary Pollen Database (MCQPD, 2001). After digitizing published

pollen diagrams and then recalculating the pollen percentages based on the total number of terrestrial pollen types, 35 new pollen sites were added (Appendix Table S1, https://link.springer.com), covering northern and southeastern China (Figure 1). Therefore, the number of pollen records was increased from 33 in the original Chinese Quaternary Pollen database (MCQPD, 2001) to 68 in the present study. 48% of these records are raw datasets with complete pollen assemblage data and 52% are digitized data from publications. The new database significantly improves the spatial coverage of vegetation in China, enabling an improved paleoclimatic reconstruction of the LGM. The quality of the dating control for the LGM was assessed by assigning a rank from 1 to 7, using ranking schemes from the Cooperative Holocene Mapping (COHMAP) project (Webb, 1985). The dating controls for ~18% of the records are better than 3D/3C (Appendix Figure S1).

Our quantitative paleoclimatic reconstruction using an inverse vegetation model is based on biome scores compiled from the pollen data. Groups of taxa have a better-defined response to climatic changes than individual taxa (Prentice and Jolly, 2000); thus, using groups of taxa for paleoclimatic reconstruction can provide more reliable results when good analogs of fossil assemblages are lacking (Peyron et al., 1998), especially during glacial periods. In addition, the homogeneous treatment applied using the standardization of biomes to the pollen data allows global/regional paleoclimatic reconstructions for the LGM (Wu et al., 2007b). In this study, vegetation type was quantitatively reconstructed using biomization, following the classification of plant functional types (PFTs) and biome assignment in China by the Members of China Quaternary Pollen Data (MCQPD, 2001), which has been widely tested on modern pollen assemblages from surface sediments.

Modern monthly mean climate variables, including temperature, precipitation and cloudiness, were spatially interpolated for each modern pollen site based on the datasets (1951–2001) from 657 meteorological observation stations over China (Monthly surface meteorological records in China, China Climate Bureau, 1951–2001). A 2-layer back-propagation (BP) artificial neural network technique was used for interpolation. This method is more efficient than many other techniques since the results are validated by independent data sets, and therefore it has been widely applied in paleoclimatology (Guiot et al., 1996). Soil properties were derived from the digital world soil map produced by the Food and Agricultural organization (FAO) (FAO, 1995), and because of the lack of paleosol data, soil characteristics were assumed to have been the same during the LGM. Atmospheric CO_2 concentration for the LGM was taken from ice core records (EPICA community members, 2004) and set at 200 ppmv.

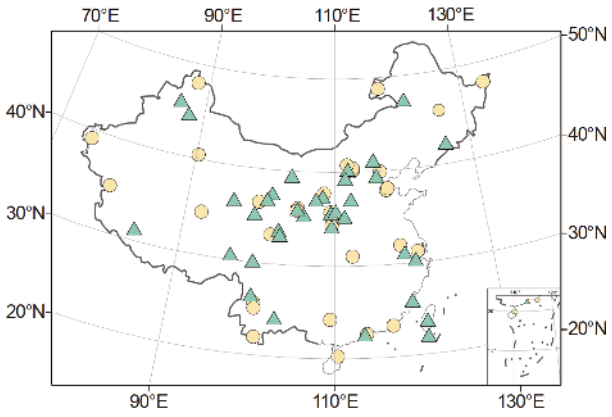

Figure 1 Distribution of LGM pollen sites in China. Circles represent records from the original China Quaternary Pollen Database, and the triangles represent new pollen sites in this study.

2.2 Inverse vegetation model

Inverse Vegetation Model, which is highly dependent on the BIOME4 model (Kaplan, 2001), is used in our reconstruction (Figure 2). The principle behind this method is that, using an iterative approach, a representative set of climate scenarios compatible with the vegetation records (i.e., biome scores at the pollen collection site) is identified within the climate space and constructed by systematically perturbing the input variables (e.g. *atmospheric* CO_2 *concentration*, *soil*, ΔT, ΔP) of the model (Table 1). The IVM provides the possibility, for the first time, to reconstruct both annual and seasonal climates for the LGM over China. Moreover, it offers a means of evaluating the impact of atmospheric CO_2 concentration on competition between plant growths, and thus it increases the reliability of pollen-based reconstructions. More detailed information about the IVM method can be found in Guiot et al. (2000) and Wu et al. (2007a).

As plant growth is constrained by climatic conditions, especially bioclimatic conditions, our aim is to reconstruct the bioclimatic variables, including growing degree-days above 5°C (GDD), mean temperature of the coldest month (MTCO), mean temperature of the warmest month (MTWA), and the ratio of actual to potential evapotranspiration (α), that constrain vegetation composition and therefore pollen assemblages. In order to facilitate comparison with previous climate studies, other variables such as mean annual temperature (ANNT) and precipitation (ANNP) are also estimated based on the monthly variables. Thus, the IVM method can reconstruct not only the seasonal variation but also the annual mean climatic state.

In order to improve paleoclimate reconstructions for glacial periods based on pollen data, it is necessary to take into account the direct physiological impact of low CO_2 concentrations on vegetation. The inverse modeling method enables us to solve part of this problem by reconstructing the

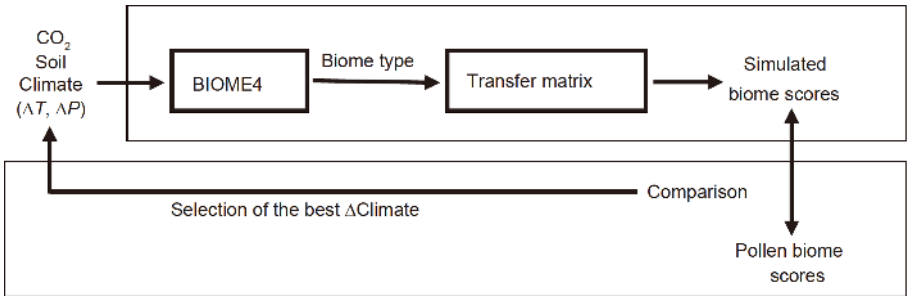

Figure 2 Schematic diagram of the inverse vegetation modelling approach for paleoclimate reconstruction (Wu et al., 2016).

Table 1 Ranges of input parameters used for the LGM paleoclimatic reconstruction[a)]

Parameter	Range
ΔT_{jan}	[–30, 10]°C
ΔT_{jul}	[–30, 10]°C
ΔP_{jan}	[–90, 100]%
ΔP_{jul}	[–90, 100]%
CO_2	200 ppmv
Iterative number	10000

a) The ranges are expressed as anomalies from modern values (deviation for temperature and percentages for precipitation).

probability distribution of LGM climates under different CO_2 concentrations and to identify potential climates that explain the occurrence of a paleo-ecosystem. To evaluate the effects of CO_2 levels on the pollen-based paleoclimatic reconstructions, we devised two experiments. LGM340: an experiment with modern atmospheric CO_2 concentration of 340 ppmv; LGM200: an experiment with LGM atmospheric CO_2 concentration of 200 ppmv.

3. Results

3.1 Biome distribution in China at the LGM

The pattern of change in biome distribution during the LGM period (Figure 3) exhibits a notable southeastwards expansion of steppe vegetation, which reached the present-day temperate deciduous forest (TEDE) zone near the middle and lower reaches of the Yangtze River (~32°N). Desert (DESE) was dominant in northwest China and in the western part of the Tibetan Plateau. The forest vegetation in eastern China retreated significantly southwards, and tropical seasonal forest (TSFO) was possibly absent. The northern boundary of the broadleaved evergreen/warm mixed forest (WAMF) shifted southwards as far as ~23.5°N, a shift of ~10° in latitude relative to today. The TEDE also retreated southwards to ~31°N and extended into the subtropical zone, with a position ~10° further south compared to today. These results indicate that the spatial pattern of vegetation in China has

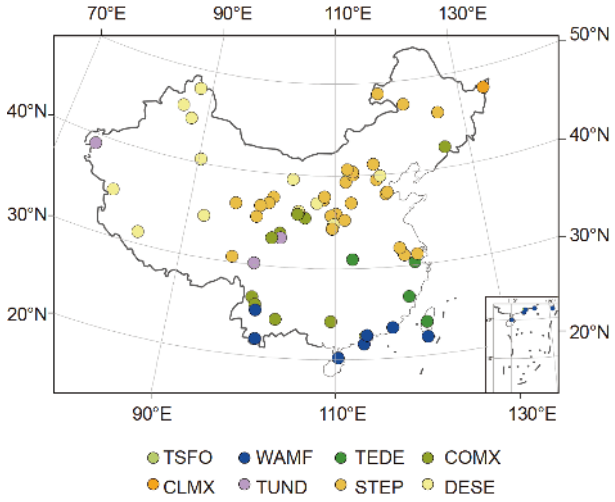

Figure 3 The spatial pattern of biomes distribution in China at the LGM. TSFO, tropical seasonal forest; WAMF, broadleaved evergreen/warm mixed forest; TEDE, temperate deciduous forest; COMX, cool mixed forest; CLMX, cold mixed forest; TUND, tundra; STEP, steppe; DESE, desert.

experienced significant changes since the LGM, as a result of global climate changes.

3.2 Climate change across China at the LGM

Paleoclimatic reconstructions are presented as maps of climate anomalies (Figure 4). The results show that at most of the sites the temperatures during the LGM period were significantly different from modern values. ANNT was ~5.6 ±0.8°C colder than today (Figure 4a), and there are anomalies of ~6.3±1.0 and ~5.5±0.5°C for northern and southern China, respectively, which are defined on the basis of the latitudinal boundary of 32°N. MTCO values were ~11.0 ±1.6°C colder than today (Figure 4b), with a significant decrease in both northern (~12.0±1.7°C) and southern China (~10.8±1.0°C). MTWA values were only ~2.6±0.9°C cooler, but the spatial pattern of MTWA is more heterogeneous than MTCO values. Eastern China was characterized by significant summer cooling, while the marginal zone of the Tibetan Plateau was less cool or similar to today (Figure 4c).

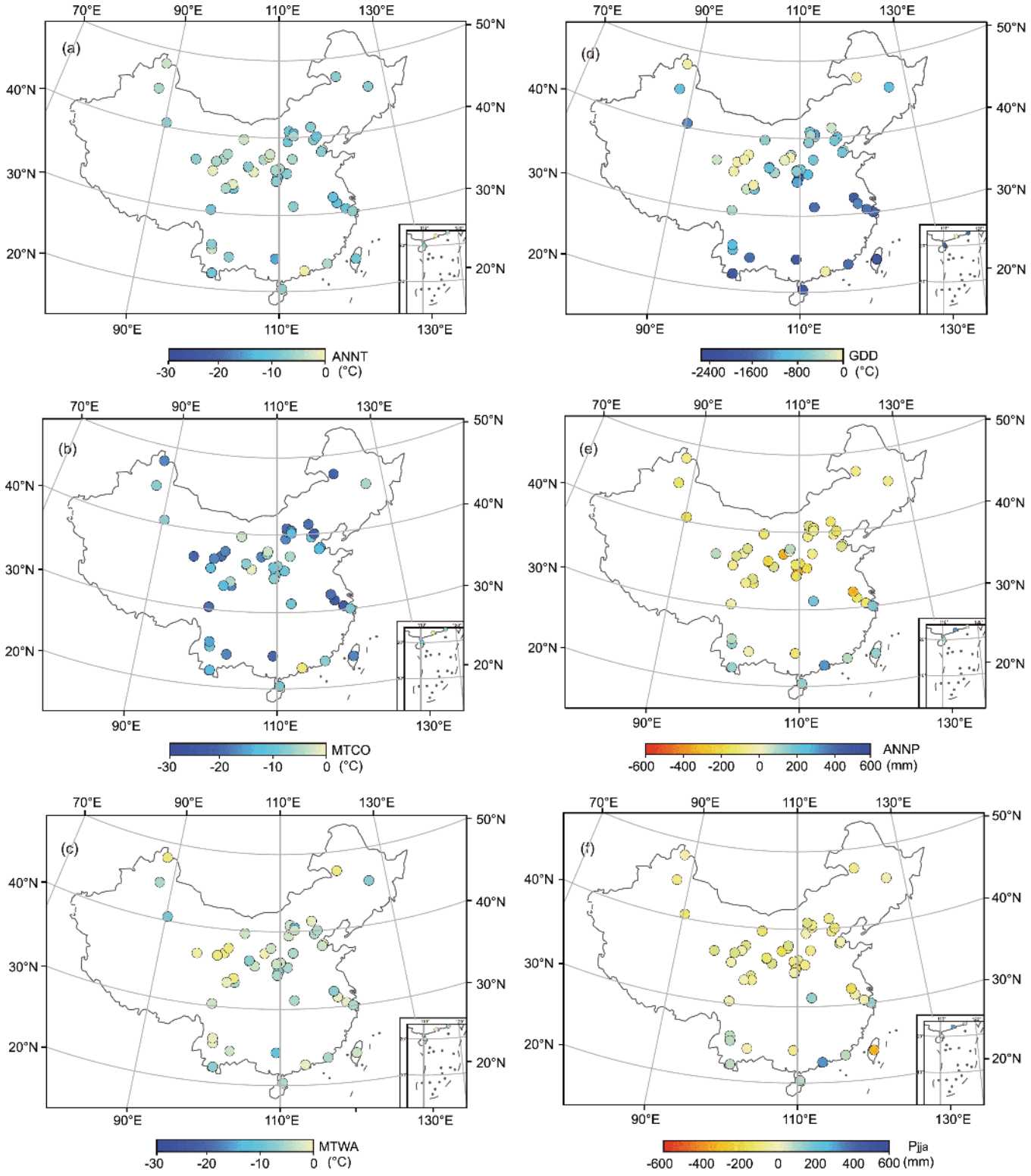

Figure 4 Reconstruction of temperature and precipitation anomalies at the LGM in China (anomalies from the mean climate during 1951–2001). (a) Mean annual temperature (ANNT); (b) mean temperature of the coldest month (MTCO); (c) mean temperature of the warmest month (MTWA); (d) growing degree-days above 5°C (GDD); (e) mean annual precipitation (MAP); (f) summer (June, July and August) precipitation (P_{jja}).

ANNT anomalies are intermediate between MTCO and MTWA, mainly due to winter temperature cooling. GDD decreases were ~962.3±130.3°C, and the pattern of GDD anomalies is similar to that of MTWA, with a maximum reduction of ~1616.0±288.4°C in southern China and a minimum reduction of ~650.3±107.7°C in northern China

(Figure 4d).

Reconstructed precipitation anomalies show a substantially different pattern compared to the temperature anomalies. The climate in China was generally drier than today (Figure 4e); there was a maximum decrease of ~51.2±21.4 mm in northern China, while a similar pattern to today (decrease of ~0.2±41.5 mm) occurred in southern China, and conditions slightly wetter than today occurred in the Hengduan Mountains and the coastal areas in southern China. ANNP anomalies are attributed mainly to summer rainfall decreases based on the seasonality of precipitation changes (Figure 4f).

3.3 Effect of CO_2 on climate reconstruction at the LGM

In order to evaluate the effect of different atmospheric CO_2 concentrations (i.e., 200 ppmv and 340 ppmv) on climatic reconstruction at a regional scale during the LGM, we integrated the bioclimatic probability distributions of all pollen sites for both northern and southern China. The results are illustrated in Figure 5.

The sensitivity experiments using various CO_2 concentrations indicate that the reconstructions of ANNT, ANNP, MTCO, MTWA and GDD for the lower CO_2 level of the LGM are similar to the distribution under the higher CO_2 concentration at present. The results reveal that the vegetation changes in China were less responsive to the CO_2 level than climate changes during glacial-interglacial periods.

4. Discussion

Previous studies showed that the ANNT of China was ~8–10°C colder than today (Appendix Table S2); in addition, the changes exhibited a striking geographical pattern, including cooling of ~2–7°C in southern China, ~8–10°C in northern and northeastern China, ~6–9°C on the Tibetan Plateau, and up to ~13–15°C in the Hexi Corridor of northwestern China (Jiang et al., 2011). Although the direction of changes in our climatic reconstructions are generally in agreement with previous studies, the ANNT of China in this study is ~5.6 ±0.8°C colder than today, which is less than the previous estimates (Figure 6), especially in northern China. In addition, our climate reconstruction for the LGM exhibits a more pronounced seasonal variation than today: the MTCO and MTWA are lowered by ~11.0±1.6 and ~2.6±0.9°C, respectively. Our MTCO reconstruction is also consistent with that based on of sand-wedge proxies in the Hexi Corridor, suggesting that this proxy mainly reflects a decrease in winter temperature (Appendix Table S3).

The hydrological anomalies reconstructed in the present

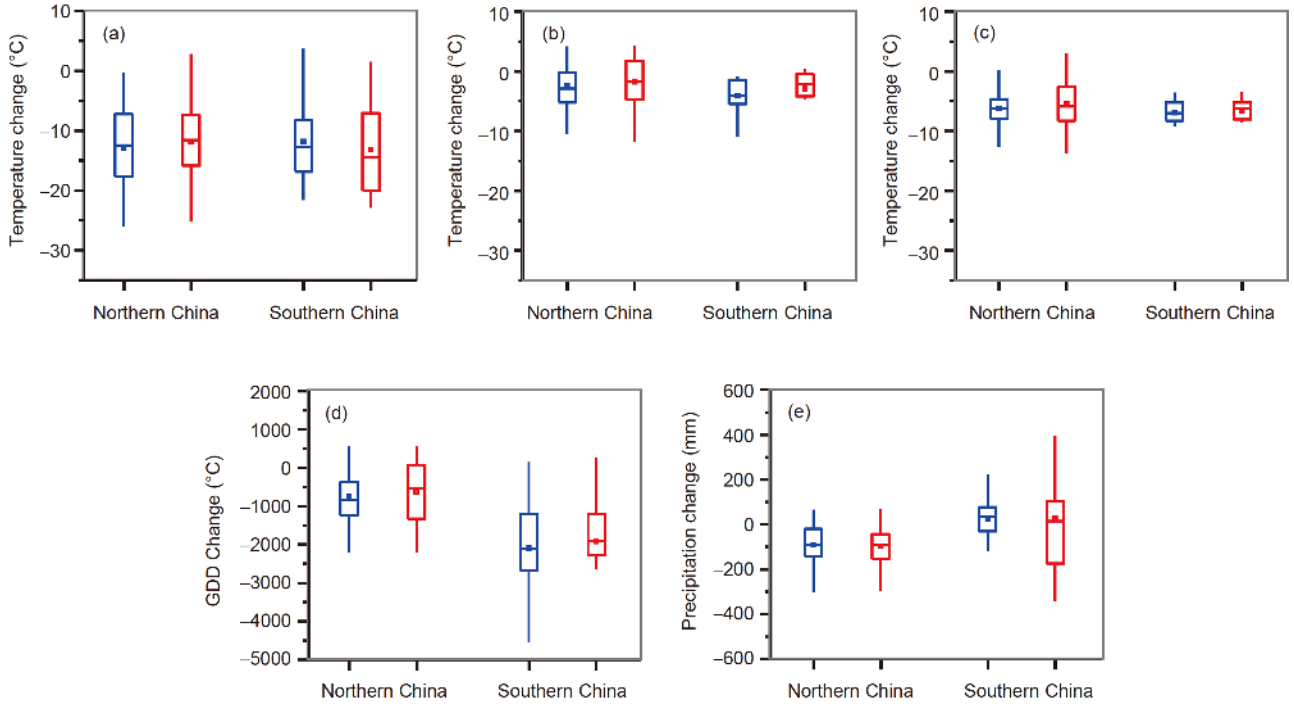

Figure 5 The effect of different atmospheric CO_2 levels on paleoclimatic reconstruction at the LGM. (a) Mean temperature of the coldest month (MTCO); (b) mean temperature of the warmest month (MTWA); (c) mean annual temperature (ANNT); (d) growing degree-days above 5°C (GDD); (e) mean annual precipitation (ANNP). The results for the climate reconstruction with an atmospheric CO_2 concentration of 200 ppmv is shown in blue, and the red for the climate reconstruction with an atmospheric CO_2 concentration of 340 ppmv. The boxes indicate interquartile intervals (25th and 75th percentiles), and the bars are 90% intervals (5th and 95th percentiles).

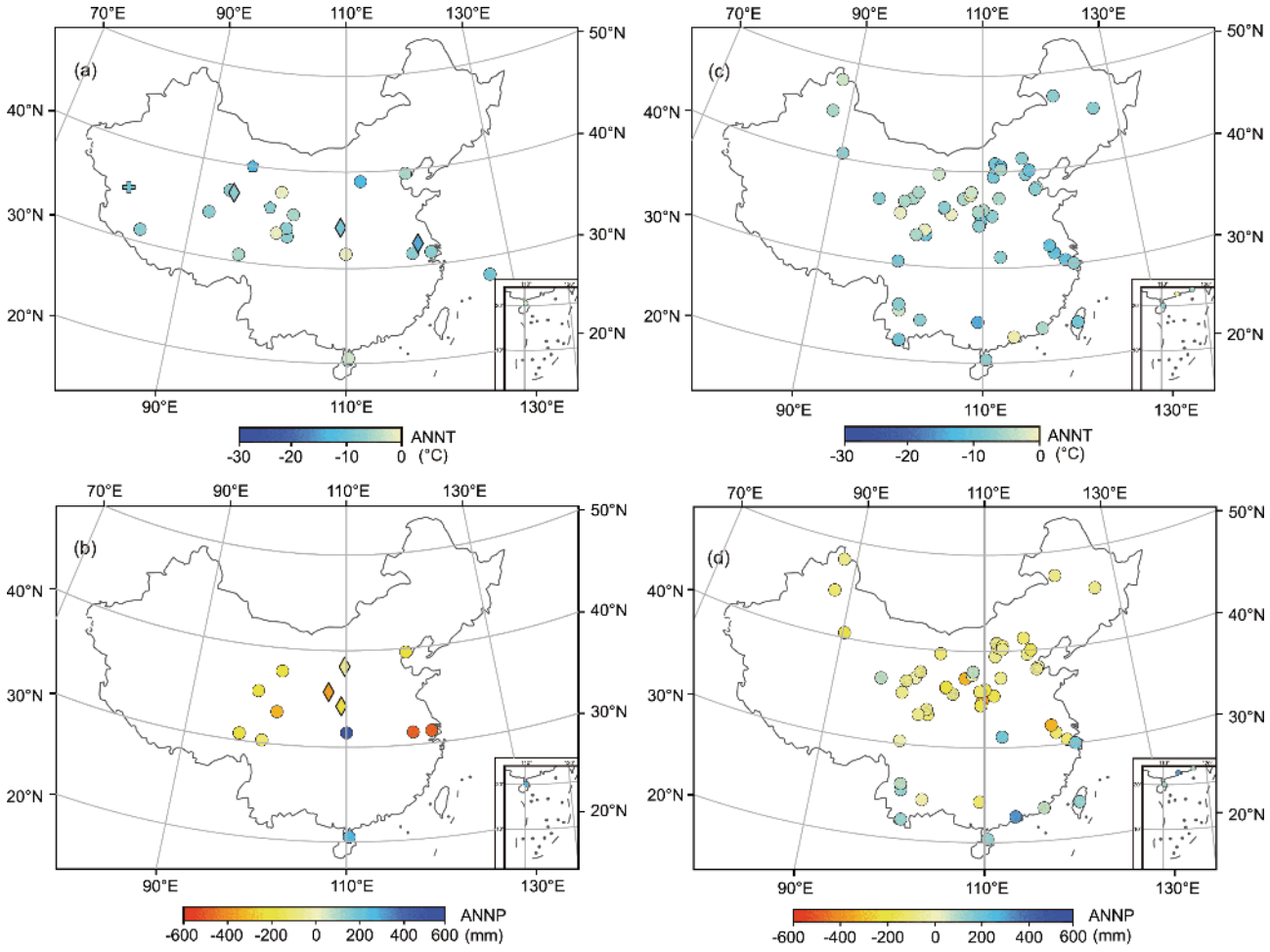

Figure 6 Comparison of the climate reconstruction of the present study with previous results. (a) Mean annual temperature (ANNT) of previous reconstructions; (b) mean annual precipitation (MAP) of a previous reconstruction; (c) ANNT reconstruction in this study; (d) ANNP reconstruction in this study. Qualitative reconstructions are based on pollen (circle), paleo-sand wedges (pentagons), oxygen isotope records of ice cores (crosses), oxygen isotope records of stalagmites, soils, and environmental magnetic properties (diamonds).

study are generally smaller (wetter) than previous estimates (Figure 6b), notably for ANNP. Previous reconstructions were drier than ~208 mm compared to today in the case of most of the records distributed in northern China, whereas our reconstructions indicate moister climates with an ANNP decrease of only ~51.2±21.4 mm.

A major difference between previous statistical methods and the IVM approach is that the former approach is calibrated for pollen originating from plants growing under modern levels of atmospheric CO_2 (~340 ppmv); by contrast, the inverse modeling does not require such a calibration, since the atmospheric CO_2 concentration is a model parameter. Our sensitivity analysis revealed that the climate reconstructions in China were less responsive to the decrease in CO_2 level (from 340 to 200 ppmv) than to climate change. Our results are in accord with previous findings for North America (Izumi and Bartlein, 2016) which indicate that CO_2 did not significantly affect temperature reconstructions during the LGM period; however, they disagree with studies of Europe and Eurasia (Wu et al., 2007b) where the effect of the low CO_2 concentration on temperature and precipitation reconstructions at the LGM was substantial. These findings reveal that the effect of CO_2 on pollen-based LGM reconstructions differs by vegetation type, which has a high degree of spatial variability.

Comparison of our results with those of previous paleoclimatic reconstructions reveals the following: First, our results provide superior quantitative climate estimates with a more detailed spatial resolution; this is because the number of pollen sites used is significantly increased for the LGM, especially the data provision for previous geographical gaps. Second, previous reconstruction methods are based on the assumption that modern vegetation-climate interactions remain constant through time, and implicitly assume that these interactions are independent of changes in seasonal temperature and precipitation. Thus, it is difficult to determine the relative influences of these various factors on plant growth, and therefore vegetation changes are mainly attrib-

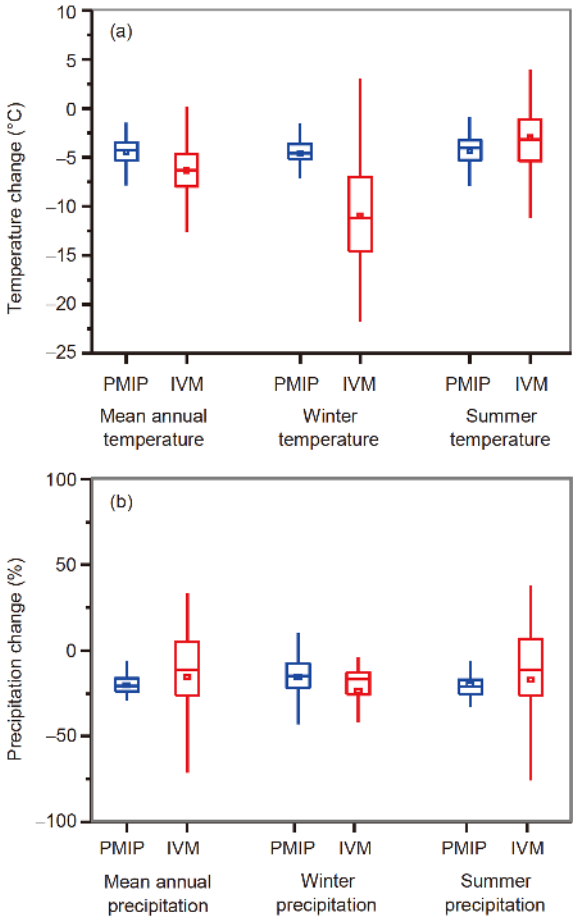

Figure 7 Comparison of the climate reconstructions of the present study and model simulations. (a) Temperature change; (b) precipitation change; PMIP: paleoclimate model simulations; IVM: inverse vegetation model. The winter season is from December to February and the summer season is from June to August. The boxes indicate interquartile intervals (25th and 75th percentiles), and the bars are 90% intervals (5th and 95th percentiles).

uted to a single climatic factor. This may be responsible for the larger values of the temperature and precipitation reconstructions in the previous studies compared with our IVM approach. By contrast, the IVM method can reveal how changes in seasonal climate account for the observed distribution of vegetation changes at the LGM; in addition, the *priori* distribution of the input climate parameters (Table 1) spans the entire possible climate space at the LGM, enabling us to achieve a quantitative paleoclimatic reconstruction. Therefore, the IVM approach can improve the understanding of paleoclimatic reconstruction on the relationship between paleoclimate and palaeovegetation from statistical method to physiological process-based model (Guiot et al., 2000; Wu et al., 2007a, 2007b).

In recent years, great efforts have been made by the modeling community (e.g. PMIP) to the design of LGM experiments using similar boundary conditions (Pinot et al., 1999; Otto-Bliesner et al., 2009; Braconnot et al., 2012; Harrison et al., 2015). Progress in understanding the LGM climate and its spatial variability can be made by comparing large-scale simulations by global climate models. The decrease of ANNT in China evident in PMIP simulations (based on 34 models) was ~4.5°C (Jiang et al., 2011, Tian and Jiang, 2016), and is slightly less than our reconstruction of ~5.6±0.8°C (Figure 7a). However, in terms of the seasonal variations, the MTCO decrease of ~11.0±1.6°C in our reconstruction is substantially colder than the simulated winter temperature of ~4.5°C; while the MTWA cooling of ~2.6 ±0.9°C of our study is slightly lower than the simulated summer temperature of ~3.8°C (Figure 7a). This suggests that the model simulations fail to reproduce the seasonal temperature pattern reconstructed by pollen data. In addition, the spatial variation of precipitation (%) in our reconstructions are broadly consistent with the model simulations, which is significantly decrease in northern China while is less dry in southern China. The reconstructed decrease in ANNP of ~46.3±17.8 mm is much lower than the model simulation of a decrease of ~144 mm. Although the model simulation of winter precipitation is consistent with the IVM reconstruction of a ~15% decrease, the summer precipitation decrease of ~21% is higher than the reconstructed result of ~11% (Figure 7b); this is the reason for the difference in ANNP between the model simulations and our reconstructions.

The foregoing results reveal that although the mean annual climate from model simulations is broadly spatially consistent with that of paleoclimate reconstructions, there is still a large divergence in terms of the seasonal variations. Our results highlight the importance of improving the seasonal climatic simulation in future paleoclimate models.

The divergence between the results of the two approaches may also be related to the lower spatial resolution of the existing models, which cannot therefore provide a reliable climate simulation for the complex terrain of China. Thus, a next step in improving the performance of model simulations is to increase their spatial resolution (Hostetler et al., 1994; Ju et al., 2007). In addition, due to their limitations the existing models do not include all of the dynamic processes of the Earth's climate system (Braconnot et al., 2007; Hargreaves et al., 2013), which reduces the accuracy of their climate simulations, especially in terms of seasonality. In addition, we also need to improve seasonal paleoclimatic reconstructions. Although the IVM method can reconstruct seasonal climate changes, the approach relies mainly on the BIOME4 vegetation model. Thus, it is important to improve its vegetation simulation of the East Asian monsoon region, and further verification is needed by adapting this approach to other vegetation models. In the future, comparison of paleoclimate reconstructions with model simulations at different times and spatial scales, together with enhancing the ability of model simulations of the past, can potentially improve our ability to predict future climate changes using

models of Earth's climate system.

5. Conclusion

We have used an improved inverse vegetation model based on physiological processes, combined with an augmented China Quaternary Pollen Database, to produce new quantitative paleoclimate reconstructions for the LGM in China. Our results confirm the ability of the IVM method to provide spatially coherent paleoclimatic patterns for the LGM in China and they indicate that the lower atmospheric CO_2 concentration of the LGM has little effect on the paleoclimate reconstructions. ANNT, MTCO and MTWA during the LGM in China were lower by ~5.6±0.8, ~11.0±1.6 and ~2.6 ±0.9°C, respectively, than today; in addition, the climate had a more strongly developed seasonal pattern. The changes of ANNT were mainly due to the decrease of MTCO. ANNP was ~46.3±17.8 mm lower than today, especially in northern China, due to the decrease in summer rainfall. Comparison with paleoclimate model simulations indicates that although most of the models are in broad agreement with the mean annual climate changes, there are still large divergences in terms of the seasonal climate. Our results suggest that it is crucially importance to improve the seasonal paleoclimate simulations of the models, as well as to improve the quality of paleoclimate reconstructions based on proxy records from geological archives.

Acknowledgements *Special acknowledgement is due to the China Quaternary Pollen Data Base for providing the 33 pollen records used in this study. This study was supported by the Strategic Priority Research Program of the Chinese Academy of Sciences (Grant No. XDA13010106), the National Key Research and Development Program of China (Grant No. 2016YFA0600504), the National Natural Science Foundation of China (Grant Nos. 41572165, 41430531, 41125011 & 41472319), and the Strategic Priority Research Program of the Chinese Academy of Sciences (Grant No. XDA05120700).*

References

Bartlein P J, Harrison S P, Brewer S, Connor S, Davis B A S, Gajewski K, Guiot J, Harrison-Prentice T I, Henderson A, Peyron O, Prentice I C, Scholze M, Seppä H, Shuman B, Sugita S, Thompson R S, Viau A E, Williams J, Wu H B. 2011. Pollen-based continental climate reconstructions at 6 and 21 ka: A global synthesis. Clim Dyn, 37: 775–802

Braconnot P, Harrison S P, Kageyama M, Bartlein P J, Masson-Delmotte V, Abe-Ouchi A, Otto-Bliesner B, Zhao Y. 2012. Evaluation of climate models using palaeoclimatic data. Nat Clim Change, 2: 417–424

Braconnot P, Otto-Bliesner B, Harrison S, Joussaume S, Peterchmitt J Y, Abe-Ouchi A, Crucifix M, Driesschaert E, Fichefet T, Hewitt C D, Kageyama M, Kitoh A, Laîné A, Loutre M F, Marti O, Merkel U, Ramstein G, Valdes P, Weber S L, Yu Y, Zhao Y. 2007. Results of PMIP2 coupled simulations of the Mid-Holocene and Last Glacial Maximum-Part 1: Experiments and large-scale features. Clim Past, 3: 261–277

Chen F H, Xu Q H, Chen J H, Birks H J B, Liu J B, Zhang S R, Jin L Y, An C B, Telford R J, Cao X Y, Wang Z L, Zhang X J, Selvaraj K, Lu H Y, Li Y C, Zheng Z, Wang H P, Zhou A F, Dong G H, Zhang J W, Huang X Z, Bloemendal J, Rao Z G. 2015. East Asian summer monsoon precipitation variability since the last deglaciation. Sci Rep, 5: 11186

Chu G Q, Sun Q, Zhu Q Z, Shan Y B, Shang W Y, Ling Y, Su Y L, Xie M M, Wang X S, Liu J Q. 2017. The role of the Asian winter monsoon in the rapid propagation of abrupt climate changes during the last deglaciation. Quat Sci Rev, 177: 120–129

Project Members C. 1976. The surface of the ice-age Earth. Science, 191: 1131–1137

Crucifix M, Harrison S, Brierley C. 2012. Recent and deep pasts in paleoclimate model intercomparison project. Eos Trans AGU, 93: 539

EPICA community members. 2004. Eight glacial cycles from an Antarctic ice core. Nature, 429: 623–628

Farrera I, Harrison S P, Prentice I C, Ramstein G, Guiot J, Bartlein P J, Bonnefille R, Bush M, Cramer W, von Grafenstein U, Holmgren K, Hooghiemstra H, Hope G, Jolly D, Lauritzen S E, Ono Y, Pinot S, Stute M, Yu G. 1999. Tropical climates at the Last Glacial Maximum: A new synthesis of terrestrial palaeoclimate data. I. Vegetation, lake-levels and geochemistry. Clim Dyn, 15: 823–856

Food and Agriculture Organization (FAO). 1995. Soil map of the world 1:5000000. Paries: U.N. Education Science and Culture Organization

Guiot J, Cheddadi R, Prentice I C, Jolly D. 1996. A method of biome and land surface mapping from pollen data: Application to Europe 6000 years ago. Palaeoclim-Data Model, 1: 311–324

Guiot J, Hély-Alleaume C, Wu H, Gaucherel C. 2008. Interactions between vegetation and climate variability: What are the lessons of models and paleovegetation data. Comptes Rendus Geosci, 340: 595–601

Guiot J, Torre F, Jolly D, Peyron O, Boreux J J, Cheddadi R. 2000. Inverse vegetation modeling by Monte Carlo sampling to reconstruct palaeoclimates under changed precipitation seasonality and CO_2 conditions: Application to glacial climate in Mediterranean region. Ecol Model, 127: 119–140

Hargreaves J C, Annan J D, Ohgaito R, Paul A, Abe-Ouchi A. 2013. Skill and reliability of climate model ensembles at the last glacial maximum and mid-Holocene. Clim Past, 9: 811–823

Harrison S P, Bartlein P J, Izumi K, Li G, Annan J, Hargreaves J, Braconnot P, Kageyama M. 2015. Evaluation of CMIP5 palaeo-simulations to improve climate projections. Nat Clim Change, 5: 735–743

Hostetler S W, Giorgi F, Bates G T, Bartlein P J. 1994. Lake-atmosphere feedbacks associated with paleolakes Bonneville and Lahontan. Science, 263: 665–668

IPCC. 2013. Climate Change: The Physical Science Basis. Cambridge: Cambridge University Press. 350

Izumi K, Bartlein P J. 2016. North American paleoclimate reconstructions for the Last Glacial Maximum using an inverse modeling through iterative forward modeling approach applied to pollen data. Geophys Res Lett, 43: 10965–10972

Jackson S T, Williams J W. 2004. Modern analogs in quaternary paleoecology—Here today, gone yesterday, gone tomorrow? Annu Rev Earth Planet Sci, 32: 495–537

Jiang D, Lang X, Tian Z, Guo D. 2011. Last glacial maximum climate over China from PMIP simulations. Palaeogeogr Palaeoclimatol Palaeoecol, 309: 347–357

Jolly D, Haxeltine A. 1997. Effect of low glacial atmospheric CO_2 on tropical African montane vegetation. Science, 276: 786–788

Joussaume S, Taylor K. 1999. The paleoclimate modeling intercomparison project. In: Braconnot P, ed. Paleoclimate Modelling Intercomparison Project (PMIP). WCRP, Canada, La Huardie`re: Proceedings of the Third PMIP Workshop. 9–24

Ju L X, Wang H J, Jiang D B. 2007. Simulation of the Last Glacial Maximum climate over East Asia with a regional climate model nested in a general circulation model. Palaeogeogr Palaeoclimatol Palaeoecol, 248: 376–390

Kageyama M, Albani S, Braconnot P, Harrison S P, Hopcroft P O, Ivanovic R F, Lambert F, Marti O, Peltier W R, Peterschmitt J Y, Roche D M, Tarasov L, Zhang X, Brady E C, Haywood A M, LeGrande A N, Lunt D

J, Mahowald N M, Mikolajewicz U, Nisancioglu K H, Otto-Bliesner B L, Renssen H, Tomas R A, Zhang Q, Abe-Ouchi A, Bartlein P J, Cao J, Li Q, Lohmann G, Ohgaito R, Shi X X, Volodin E, Yoshida K, Zhang X, Zheng W P. 2017. The PMIP4 contribution to CMIP6—Part 4: Scientific objectives and experimental design of the PMIP4-CMIP6 Last Glacial Maximum experiments and PMIP4 sensitivity experiments. Geosci Model Dev, 10: 4035–4055

Kaplan J O. 2001. Geophysical applications of vegetation modeling. Doctoral Dissertation. Lund: Lund University

Liu Z Y, Zhu J, Rosenthal Y, Zhang X, Otto-Bliesner B L, Timmermann A, Smith R S, Lohmann G, Zheng W P, Timm O E. 2014. The Holocene temperature conundrum. Proc Natl Acad Sci USA, 111: E3501–E3505

MARGO Project Members. 2009. Constraints on the magnitude and patterns of ocean cooling at the Last Glacial Maximum. Nature Geosci, 2: 127–132

Members of China Quaternary Pollen Data Base (MCQPD). 2000. Pollen-based biome reconstruction at Middle Holocene (6 ka BP) and Last Glacial Maximum (18 ka BP) in China (in Chinese with English Abstract). Acta Bot Sin, 42: 1201–1209

Members of China Quternary Pollen Data Base (MCQPD). 2001. Simulation of China biome reconstruction based on pollen data from surface sediment sample (in Chinese with English Abstract). Acta Bot Sin, 43: 201–209

Otto-Bliesner B L, Schneider R, Brady E C, Kucera M, Abe-Ouchi A, Bard E, Braconnot P, Crucifix M, Hewitt C D, Kageyama M, Marti O, Paul A, Rosell-Melé A, Waelbroeck C, Weber S L, Weinelt M, Yu Y. 2009. A comparison of PMIP2 model simulations and the MARGO proxy reconstruction for tropical sea surface temperatures at last glacial maximum. Clim Dyn, 32: 799–815

Peyron O, Guiot J, Cheddadi R, Tarasov P, Reille M, de Beaulieu J L, Bottema S, Andrieu V. 1998. Climatic reconstruction in Europe for 18000 yr B.P. from pollen data. Quat Res, 49: 183–196

Pinot S, Ramstein G, Harrison S P, Prentice I C, Guiot J, Stute M, Joussaume S. 1999. Tropical paleoclimates at the Last Glacial Maximum: Comparison of Paleoclimate Modeling Intercomparison Project (PMIP) simulations and paleodata. Clim Dyn, 15: 857–874

Prentice I C, Jolly D. 2000. Mid-Holocene and glacial-maximum vegetation geography of the northern continents and Africa. J Biogeogr, 27: 507–519

Song C Q, Sun X J. 1997. Establishment of the transfer functions of the pollen-climatic factors in Northern China and the quantitative climatic reconstruction at DJ core (in Chinese with English Abstract). Acta Bot Sin, 39: 554–560

Street-Perrott F A, Huang Y, Perrott R A, Eglinton G, Barker P, Ben Khelifa L, Harkness D D, Olago D O. 1997. Impact of lower atmospheric carbon dioxide on tropical mountain ecosystems. Science, 278: 1422–1426

Sun X J, Wang F Y. 1996. Pollen-climate response surface of selected taxa from Northern China. Sci China Ser D-Earth Sci, 39: 486–493

Tian Z P, Jiang D B. 2016. Revisiting last glacial maximum climate over China and East Asian monsoon using PMIP3 simulations. Palaeogeogr Palaeoclimatol Palaeoecol, 453: 115–126

Wang M Y, Zheng Z, Man M L, Hu J F, Gao Q Z. 2017. Branched GDGT-based paleotemperature reconstruction of the last 30000 years in humid monsoon region of Southeast China. Chem Geol, 463: 94–102

Webb T III. 1985. A Global paleoclimatic data base for 6000 yr BP. Providence, RI(USA): Brown University, Department of Geological Sciences. 25–34

Webb T III , Anderson K H, Bartlein P J, Webb R S. 1998. Late Quaternary climate change in eastern North America. Quat Sci Rev, 17: 587–606

Wu H B, Guiot J, Brewer S, Guo Z T. 2007a. Climatic changes in Eurasia and Africa at the last glacial maximum and mid-Holocene: Reconstruction from pollen data using inverse vegetation modelling. Clim Dyn, 29: 211–229

Wu H B, Guiot J, Brewer S, Guo Z T, Peng C H. 2007b. Dominant factors controlling glacial and interglacial variations in the treeline elevation in tropical Africa. Proc Natl Acad Sci USA, 104: 9720–9724

Wu H B, Lu Y L, Jiang W Y, Li Q, Sun A Z, Guo Z T. 2016. Paleoclimate reconstruction from pollen data using inverse vegetation approach: Validation of model using modern data (in Chinese with English Abstract). Quat Sci, 36: 520–529

Zheng Z, Guiot J. 1999. A 400 000-year paleoclimate reconstruction in tropical region of China (in Chinese with English Abstract). Acta Sci Nat Univ Sunyatseni, 38: 94–98

(Responsible editor: Zhengtang GUO)